Optimizing the power hub of offshore multi-platform for oil and gas production

***Ronaldo L. A. Freire*[a], *Daniel Flórez-Orrego*[b], *Julio A. M. da Silva*[c], *Cyro Albuquerque Neto*[d] and *Silvio de Oliveira Junior*[e]**

[a] *University of São Paulo, São Paulo, Brazil, rlafreire@usp.br,* **CA**
[b] *University of São Paulo, São Paulo, Brazil, daflorezo@usp.br*
[c] *Federal University of Bahia, Salvador, Brazil, julio.silva@ufba.br*
[d] *FEI University Center, São Bernardo do Campo, Brazil, cyroan@fei.edu.br*
[e] *University of São Paulo, São Paulo, Brazil, soj@usp.br*

Abstract:

Offshore oil and natural gas production is an energy-intensive activity and is responsible for the emission of significant amounts of carbon dioxide into the atmosphere. The main emitting source is the simple-cycle gas turbines (SCGT) of the utility system which supplies heat and power to the production platforms. Severe vessel area and weight constraints are often cited as the main reason why production platforms are unable to allocate high-efficiency combined-cycle gas turbines (CCGT) common in land-based power plants. Published work suggests that in production development projects of giant offshore oil fields, the thermodynamic efficiency of the utility system may be increased significantly, without prejudice to project economic viability, through an additional vessel dedicated to generating power in CCGT. The best results are obtained when the power demand is split between the power hub and local gas turbines which are used in cogeneration mode to additionally produce heat for separation purposes. Therefore, this work proposes a methodology for optimizing the power block of the power hub. The first step is the selection of combined cycle configurations from the commercially available aero-derivative gas turbines. At sequence, evolutionary algorithms are used in the multi-objective optimization (MOO) of the steam bottoming cycle, whose objective is to obtain the configurations that produce the best results in terms of atmospheric CO_2 emissions, occupied area, and capital cost. A method is then proposed to select the best solution from the non-dominated solutions that compose the Pareto front, taking into account the constraints imposed by the vessel of the central power plant and the objectives to be optimized. The power hub solution presented average exergy efficiency 8.2p.p. above the conventional, thus reducing the fuel gas consumption by 1.74 million ton and consequently avoiding the emission of 4.75 million ton of CO_2. Finally, in the context of growing environmental concern and taxation of CO_2 emissions, this work contributes to highlighting the advantages of the central power plant in future maritime production development projects in large oil and gas fields.

Keywords:

Offshore, Power Hub, Combined-Cycle, Multi-Objective Optimization, CO_2 Emission.

1. Introduction

Offshore oil production plays a strategic role in meeting the world's energy demand. According to the U.S. Energy Information Administration, in 2015, almost a third of the world's oil production occurred at sea, with Brazil ranking as one of the top five offshore producers [1]. According to the Brazilian Agency of Petroleum, Natural Gas and Biofuels, offshore oil production represented 93% of the country's total production in 2015 [2]. Since 2006, giant offshore oil fields are being discovered in Brazil, resulting in the largest offshore production development projects today, which are characterized by clusters of production platforms.

Offshore oil production is energy intensive and significant amounts of carbon dioxide (CO_2) are released into the atmosphere by low-efficiency utility plants on production platforms. These systems typically have simple-cycle gas turbines (SCGT) due to severe area and weight restrictions on vessels.

Although equipped with waste heat recovery units (WHRU) to convert part of the flue gas energy into useful heat, the cogeneration demand is usually less than the system potential. Additionally, power and heat demands undergo profound changes throughout the platform operating life, resulting in partial load operation most of the time. The operation of rotating machines far from the best efficiency point incorporates even more inefficiencies in the power plant.

Kloster [3] indicates that the increasing commercial value of natural gas and the taxation of greenhouse gas emissions are the main factors driving the technological development of steam bottoming cycles (SBC) for offshore platforms. According to Nguyen et al. [4], the integration of SBC on offshore platforms is currently regarded as the most promising option for improving the performance of these energy-intensive systems. However, weight and area requirements are the major obstacles to SBC in real projects. A heat recovery steam generator (HRSG) may require 25-50% extra area than a WHRU [3]. Nevertheless, as the heat exchanger is placed on the top of the gas turbine main skid, the required extra area should not be a real problem.

Følgesvold et al. [5] assessed a GE LM2500+G4 gas turbine as topping cycle, and a once-through heat recovery steam generator with extraction and back-pressure steam turbines (ST) as bottoming cycles. According to the authors, the thermal efficiency could be increased by 12.3p.p. and 8.9p.p. and CO_2 emission reduced 26% and 21%, respectively, compared do the SCGT configuration. Nord, Martelli and Bolland [6] optimized the weight-to-power ratio of a SBC for offshore platform. A reduction of 4% compared to a knowledge-based design was obtained, and a Pareto front allow the designer to select the solution which best matches the installation constraints. Riboldi and Nord [7] investigated the optimum design approach for offshore SBC. Authors suggest that, rather than at peak conditions, better overall performance is obtained when designing the plant at the end-life conditions.

A power hub can be attractive in production development projects with clusters of platforms, common in giant oilfields. Some recent Brazilian pre-salt projects, such as those in the Lula, Búzios and Mero oil fields, have up to four platforms distant up to 10 km from each other. The electrical interconnection among platforms and to a power hub is technically possible and can be a solution to eliminate the area and weight constraints that currently prevent the adoption of SBC on offshore platforms.

Vidoza et al. [8] assessed a power hub connected to three pre-salt platforms. The power hub with power blocks containing three gas turbines coupled to a dual-pressure HRSG and a ST resulted in the best cost-weight ratio and 53.2% thermal efficiency. Defining the best configuration for the utility plant in a production cluster with power hub is a hard task. A hybrid solution with power generation in both production units and power hub increased the Second Law performance by 9.1p.p. in the work of Freire and Oliveira Jr [9]. An incremental financial analysis including the sensitivity to carbon taxation shows that power hubs may not only be technically, but also financially viable in the future.

This work adds to the body of knowledge a comparative analysis which includes the optimization of the SBC based on three objective functions: cost of capital, area occupied by the main equipment and atmospheric CO_2 emissions. The results obtained highlight the potential benefits of combined-cycle power generation in the power hub associated with the combined heat and power (CHP) production in the production platforms.

2. Production development project

Offshore platforms are normally equipped with SCGT-WHRU power blocks to supply efficiently heat and power to the entire vessel considering its operating life. This section defines the case study under investigation, which integrates multiple production units to a power hub equipped with CCGT power blocks to supply part of the demanded electricity.

2.1. Energy demand

Silva and Oliveira Jr. [10] estimated the lifetime energy demand of a primary processing plant in a pre-salt platform. The commercial oilfield life was set as 22-year. Authors proposed to estimate the thermal demand as for the multiplication of predicted annual oil production and specific heat consumption rates, varying according to the operating mode. Similarly, energy demand is obtained from polytropic compression equations and predicted associated gas production. Gallo et al. [11] also estimated the energy demand over a pre-salt platform life through the simulation of the primary processing plant in a commercial software. Authors used available well fluids' data and Weibull statistic models with production peak near 7.5 years since production starting and the field life of 25 years to estimate power and heat demands. This work uses the electricity and heat demand curves from Gallo et al. [11]. However, a change has been made to the original electricity to consider CO_2 compressors driven by electric motors instead of SCGT. The combined heat and power demand profile in shown in Figure 1.

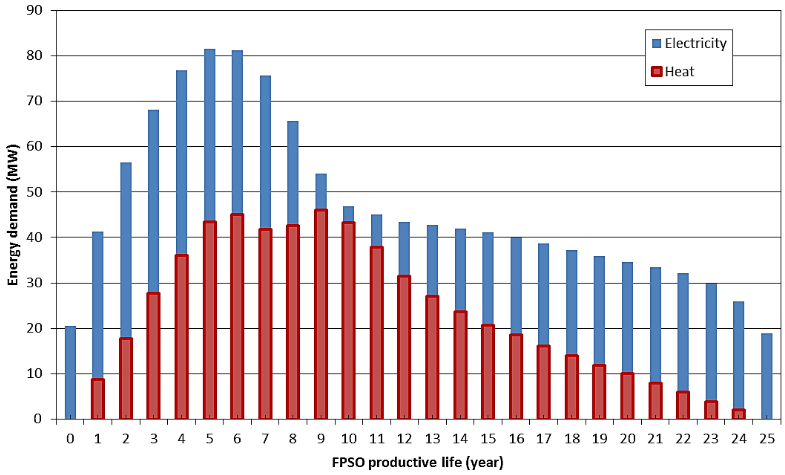

Figure 1. CHP profile of the production platform (adapted from [11])

A production development project with four identical platforms is evaluated in this work, that is, with identical heat and power as in Figure 1. In Cases 1 and 2 the start of production is delayed in 1 year and the platforms are relatively close so that the transmission losses were neglected. Figure 2 illustrate the full project taking into account the alternative design proposed in Case 2 (see item 3.1).

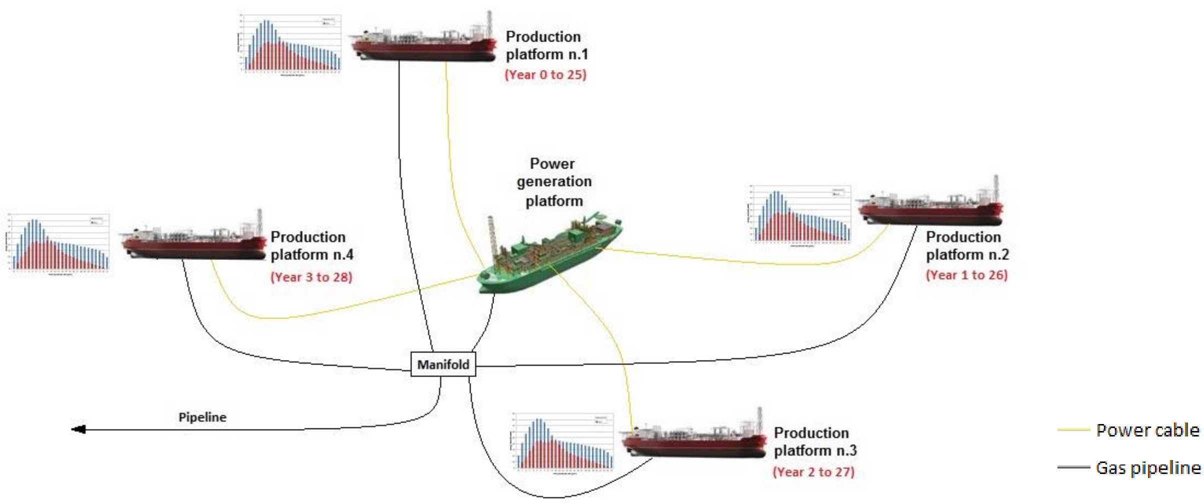

Figure 2. Production development project with four production platforms and a power hub

2.2. Fuel gas supply

The CO_2 separation in the referenced pre-salt platform occurs between 3^{rd} and 15^{th} operating year [11]. The high-pressure fuel gas is supplied by the primary processing plant within this period. In contrast, from the production starting up to the end of the 2^{nd} operating year and from the 16^{th} operating year onwards, the high-pressure fuel gas supply comes from the exporting/importing pipeline. Table 1 shows the chemical composition of the fuel gas according to its source.

Table 1. Fuel gas composition by source (% molar)

Substance	Exporting/importing pipeline (Mode A)	Internal production (Mode B)
Methane	76.05	73.72
Ethane	10.63	11.54
Propane	6.30	7.36
I-butane	0.83	1.09
Butane	1.76	1.84
I-pentane	0.22	0.29
Pentane	0.49	0.32
Hexane	0	0.05
Nitrogen	0.64	0.77
Carbon dioxide	3.08	3.00

2.3. Environmental condition in Brazilian pre-salt area

Climatological standard normals are widely used as an indicator of the conditions likely to be experienced in a given location. According to the World Meteorological Organization, climatological standard normals can be obtained through averages of climatological data calculated for consecutive 30-year periods [12]. The Brazilian Institute of Meteorology [13] provides climatological standard normals at various stations throughout the country. Cabo Frio station, localized in Rio de Janeiro state, is representative of the site conditions in the Brazilian pre-salt region. In this context, Table 2 summarizes the annual average ambient condition set for this case study.

Table 2. Climatological standard normals in Cabo Frio station: 1961-1990 [13]

Atmospheric pressure (hPa)	Ambient temperature (°C)	Relative humidity (%)
1,015	23.2	81

3. Utility plant analysis

This section is dedicated to the definition, modelling and simulation of the utility plants that support the production system defined above.

3.1. Plant configurations

The utility plant in a pre-salt facility typically has four SCGT-WHRU units to supply heat and power [10][11]. The system is configured at 4x33%, which means that the peak demand can be met by 3 power blocks, while one remains as backup for reliability reasons. This arrangement constitutes the baseline of this comparative assessment, in which the performance of the proposed system based on a power hub is evaluated. The two systems under comparison are detailed below:

- **Case 1 (baseline)**: this configuration represents the reference design case composed of a typical pre-salt production platform. Each platform has its own utility plant with 4x33% Siemens SGT-A35 aeroderivative gas turbine and waste heat recovery unit (see Figure 3);
- **Case 2 (proposal)**: a central power plant with 5x25% GE LM6000PF+ combined-cycle. Each production platform has one Siemens SGT-A35 aeroderivative gas turbine with waste heat recovery unit and 4x25% hot water boilers (HWB) (see Figure 4).

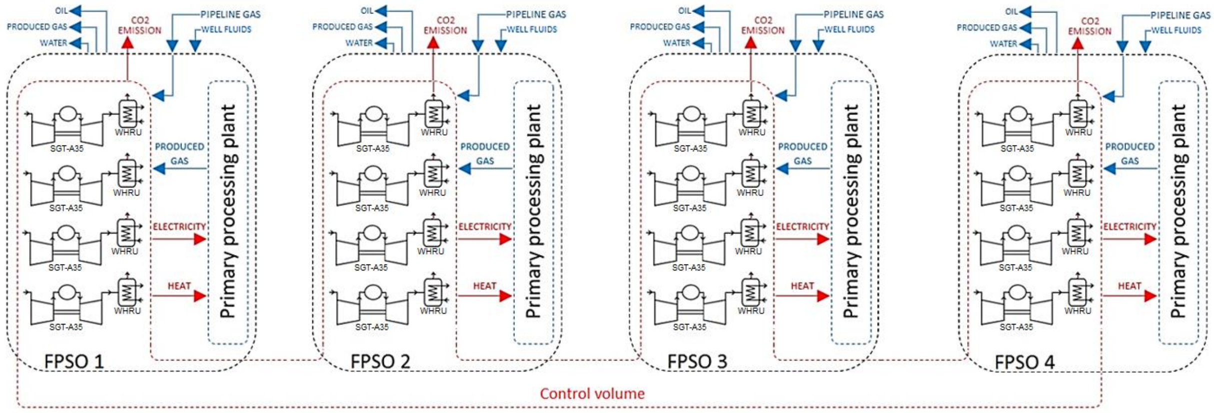

Figure 3. Schematic diagram of Case 1

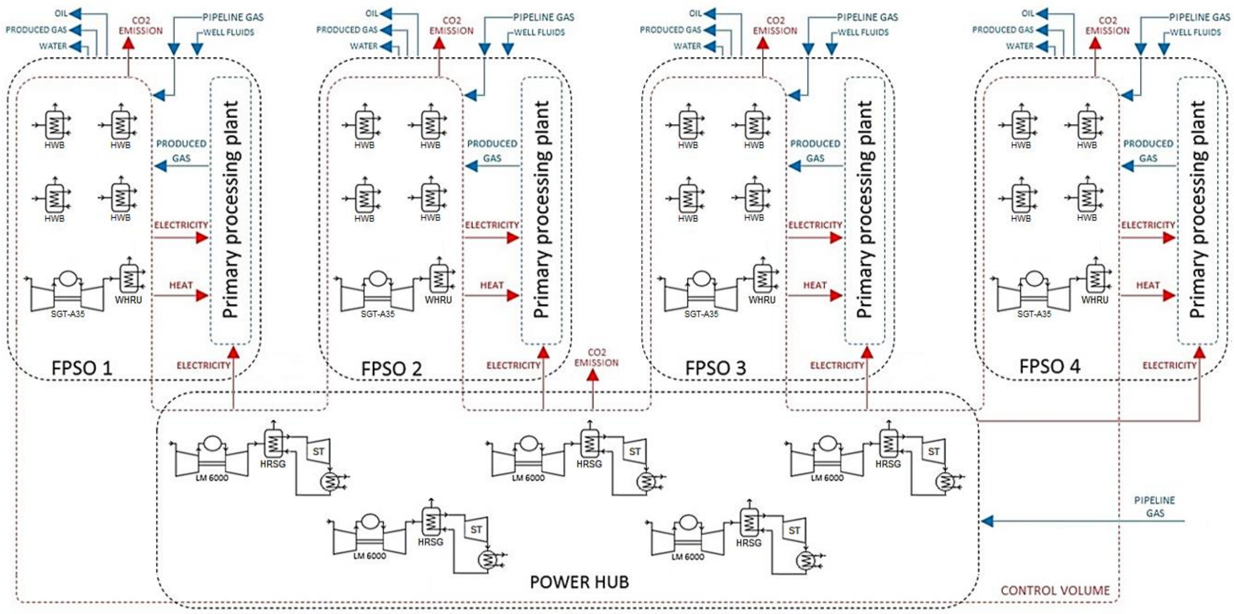

Figure 4. Schematic diagram of Case 2

3.2. Power block simulation

Utility plant processes were simulated with Thermoflow®, a comprehensive simulator suite for gas, steam and renewable power plants [14]. According to Liu and Karimi [15], Thermoflow® is one of the preferred computer programs for studying power plants. Nord, Martelli and Bolland [6] and Vidoza et al. [8] exemplify the use of Thermoflow® in the design and optimization of energy systems for offshore production. GT PRO® is used to generate cycle heat balance as well as physical design of major equipment and balance-of-plant. The off-design performance of the modelled plant is then simulated in GT MASTER® according to control set-points, loads, and ambient conditions. Modelling a power block in GT PRO® involves selecting the SCGT built-in model calibrated from manufacturers data, which is capable to simulate design and off-design performance for a given load, fuel, and environmental condition. On the other hand, WHRU is modelled from real project data and HRSG is modelled based on knowledge as no real project data is available (see Table 3). ST is multi-valve type, with 14 stages, 2.5% inlet valve pressure drop, 0.05% miscellaneous auxiliary load, 0.25% mechanical loss, 1% inlet leakage, and 90% leakage readmission.

Table 3. Design assumptions of the heat recuperator equipment

Equipment	WHRU	HRSG
Type	Simple recovery	Once-through
Arrangement	Vertical	Vertical
Pressure level	Single	Single
Pressure drop (Pa)	2400	1900
Tube arrangement	Staggered	Staggered
Tube material	ASTM A335 Gr. T11	ASTM A213 Gr. T22
Number of flow passes	16	33
Number of tubes per pass	23	30
Longitudinal pitch (mm)	110	79
Transversal pitch (mm)	127	92
Fin type	Serrated	Serrated
Fin height (mm)	11	15
Fin thickness (mm)	1.5	1
Fin spacing (mm)	3.5	3.5
Fin material	AISI 409	AISI 409

The simulation of the Siemens SGT-A35 gas turbine with waste heat recovery unit operating with fuel compositions from exporting/importing pipeline (Mode A) and internal production (Mode B) resulted in the following data (see Table 4):

Table 4. Simulated performance of Siemens SGT-A35 with waste heat recovery unit

Load (%)	25	50	75	100
Plant net power (MW)	7.36	14.83	22.22	29.51
Plant net LHV electric efficiency (%)	20.63	29.62	34.49	36.65
CHP LHV efficiency (%)	72.05	73.92	75.15	75.95
GT exhaust temperature (°C)	465	473	490	524
Stack temperature (°C)	169	180	191	204
Fuel flow – Mode A (kg/s)	0.788	1.106	1.423	1.779
Fuel flow – Mode B (kg/s)	0.789	1.107	1.424	1.780
Hot water production capacity (kg/s)	84	101	119	144
CO_2 emission - Mode A (kg/s)	2.126	2.984	3.841	4.801
CO_2 emission - Mode B (kg/s)	2.135	2.996	3.856	4.819

3.2.1. Multi-objective optimization of the GE LM6000PF+ combined-cycle

Designing SBC for offshore application is a challenging task, which involves minimizing at the same time the occupied area, capital cost and CO_2 emission. Multi-objective optimization is a multi-criterion decision-making technique used to determine the vector of design variables within the feasible region that represents the optimal solutions to a given problem, i.e., the vector of solutions that minimize or maximize simultaneously multiple functions subject to a set of constraints. Multi-objective optimization can be expressed mathematically as follows, where k is the number of objective functions $f(\vec{x})$, $\vec{x}$ is the vector of design variables, m is the number of inequality constraints $g(\vec{x})$, and p is the number of equality constraints $h(\vec{x})$.

$$\begin{aligned} Minimize&: F(\vec{x}) = \{f_1(\vec{x}), f_2(\vec{x}), \dots, f_k(\vec{x})\} \\ Subject\ to&: g_i(\vec{x}) \geq 0, \qquad i = 1,2, \dots m \\ & h_i(\vec{x}) = 0, \qquad i = 1,2, \dots p \end{aligned} \tag{1}$$

Multi-objective optimization in engineering and industry is often very challenging to solve, necessitating sophisticated techniques to tackle. Metaheuristic approaches have shown promise and popularity in recent years [16]. The genetic algorithm has been applied extensively to solve various practical industrial problems [17]. A multi-objective optimization algorithm based on NSGA-II is applied to search for the design variables vector that minimizes the following objective functions:

- Objective 1: total area per net power, m²/MW
- Objective 2: capital cost per net power, US$/kW
- Objective 3: hourly CO_2 emission per net power, kg/MWh

The optimization framework consists of interlinking GT PRO® and MATLAB® [18] to run the MOO NSGA-II algorithm. The following parameters were set: generation size 400, population size 50, crossover fraction 0.8, constraint tolerance 0.001 and function tolerance 0.0001. The design variables are steam pressure and temperature before steam turbine stop valve. The following constraints were considered in this work:

- 1000 kPa ≤ steam pressure before ST stop valve ≤ 9000 kPa abs
- 200 °C ≤ steam temperature before ST stop valve ≤ 520 °C

The MOO problem resulted in the following normalized non-dominated solutions (see Figure 5). Red, green and blue dots are the projection of the solutions (black dots) in the respective planes.

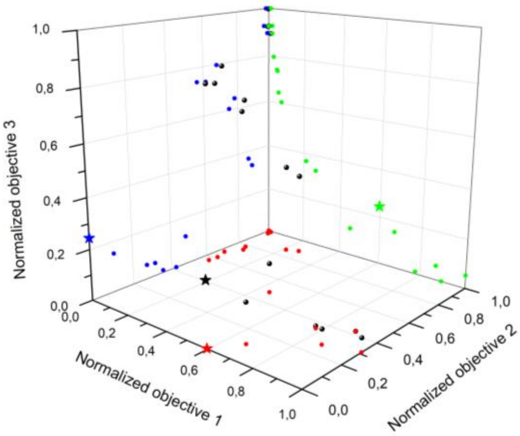

Figure 5. Pareto front solutions

Thus, the MOO was performed based on the premises and assumptions mentioned above. The design variable set that minimizes the distance between zero and normalized points is considered the solution of compromise among the non-dominated solutions that represent the trade-off between various conflicting objectives. The distance from each point to zero is calculated by the simple spatial geometry formula given below, where NOF_i means the normalized value of the $i-th$ objective.

$$Distance = \sqrt{NOF_1^2 + NOF_2^2 + NOF_3^2} \quad (2)$$

Table 5 presents the Pareto front solution that minimizes the normalized distance (which also minimizes objective 2), as well as solutions that minimize occupied area and emissions.

Table 5. Optimized SBC inlet steam pressure and temperature

Inlet steam		Obj. 1	Obj. 2	Obj. 3	Norm. obj. 1	Norm. obj. 2	Norm. obj. 3	Norm. distance
kPa (abs)	°C	m²/MW	US$/kW	kg/MW.h	-	-	-	-
2510	**458**	**2.857**	**704.4**	**409.5**	**0.60**	**0.00**	**0.24**	**0.64**
2140	436	2.842	706.8	410.1	0.90	0.42	0.00	0.99
1740	476	2.899	710.0	408.3	0.00	1.00	0.92	1.36

The solution selected (called "pseudo-optimum" because it does not eliminate the possibility of better unknown solutions) was simulated and the obtained performance is shown in Table 6. It is noteworthy that the fuel gas from the power hub is supplied only by the exporting pipeline.

Table 6. Performance of the optimized CCGT power block with GE LM6000PF+ gas turbine

Load (%)	25	50	75	100
Plant net power (MW)	20.33	35.42	47.92	61.76
GT gross power (MW)	11.92	23.72	35.36	46.88
Plant net LHV electric efficiency (%)	37.01	44.57	49.50	52.43
Fuel flow (kg/s)	1.214	1.756	2.139	2.603
GT exhaust temperature (°C)	496	532	498	512
Stack temperature (°C)	136	140	149	155
ST inlet flow (kg/s)	9.16	12.49	13.44	15.64
CO_2 emission (kg/s)	3.274	4.737	5.771	7.023

3.4. Power block operating strategy

The overall performance of SCGT plants are influenced also by its operation strategy. Riboldi and Nord [7] discussed the relationship between load and thermal efficiency in parallel CCGT operation. According to authors, the best choice for very high and low power outputs is a uniform load share between CCGT. However, in intermediate power outputs the thermal efficiency is maximized by keeping one CCGT load at high levels, while the other unit handles the remaining power output. Despite the potential benefit of operating parallel CCGT at very different load, operators normally maintain CCGT at the same load for stability reasons. This work assumes that parallel SCGT and CCGT load is equally split and the smallest amount of power blocks are operated to accomplish a certain service. Regarding to Case 2, the first level of the operating hierarchy is the SCGT in the production platform, in which the required heat governs its load. HWB supplements the hot water production when required, as well as the power hub supplies power to the production platforms.

3.5. Hot water boiler

Design and performance data of commercial HWB are hard to find in the literature. For this reason, this work assumes a simplified approach to model this equipment. A LHV thermal efficiency equal to 95% and First Law equations were used to obtain the overall off-design performance and emissions (see Table 7). The obtained results are in line with commercial HWB of similar capacity [19].

Table 7 - Hot water boiler performance

Parameter/Load (%)	25	50	75	100
Heat supply (MW)	2.88	5.75	8.62	11.50
Thermal efficiency (%)	95.0	95.0	95.0	95.0
Fuel flow – Mode A (kg/s)	0.067	0.135	0.202	0.271
Fuel flow – Mode B (kg/s)	0.067	0.135	0.202	0.271
CO_2 emission - Mode A (kg/s)	0.183	0.367	0.551	0.734
CO_2 emission - Mode B (kg/s)	0.182	0.366	0.550	0.733

3.6. Exergy efficiency and carbon emission

The exergy of flows was calculated for the reference environment and standard chemical exergy proposed by [20]. The exergy effects caused by nuclear, magnetic, electric, and surface tension forces were neglected due to its irrelevance to the case study. The specific exergy b is defined as the sum of the following exergy components: potential b_{pot}, kinetic b_{kin}, thermomechanical or physical b_{ph}, and chemical b_{ch}, according to equation (1).

$$b = b_{pot} + b_{kin} + b_{ph} + b_{ch} \tag{1}$$

There are some definitions in the literature to calculate the exergy efficiency of a given energy conversion process. The exergy efficiency of the power and heat system on offshore platforms can be determined by equation (2).

$$\eta_{ex} = \frac{\text{Useful exergy effect}}{\text{Driving exergy}} = \frac{\dot{B}_{el} + \dot{m}_w\left(b_w^{out} - b_w^{in}\right)}{\dot{m}_f b_f} \tag{2}$$

The lifespan exergy efficiency of the utility plant configurations is shown in Figure 6. A continuous increase in the exergy efficiency of the conventional plant (Case 1) is observed following the behaviour of the thermal demand curve (see Figure 1).

4. Results

The performance indicators of the conventional pre-salt platform (Case 1) and the proposed power hub (Case 2) are summarized in Table 8. Case 2 presented Second Law efficiency throughout the oilfield lifespan 8.2p.p. above Case 1, thus reducing the fuel gas consumption and increasing the exportation of natural gas by 1.74 million ton and avoiding the CO_2 emission by 4.75 million ton.

Based on Figure 6, one can note that exergy efficiency of Case 1 varies significantly compared to Case 2 in the production beginning as well as when the oilfield becomes mature. Generically, Case 1 is characterized by decentralized plants prone to partial load operation, whereas Case 2 benefits either by a relatively flat HWB efficiency and power blocks operation closer to the design point. For instance, the largest exergy efficiency gap occurs in the 25th year (16.3p.p.), when Case 1 has six SCGT-WHRU power blocks with average load of 60.3%, whereas Case 2 has two CCGT power blocks at 86.4% average load to supply the entire power demand and HWB for heat purposes.

Table 8 – Utility plant performance indicators comparison throughout the oilfield lifespan

Key performance indicator	Case 1	Case 2
Average exergy efficiency (%)	35.8	44.0
Overall fuel gas consumption (10^6 ton)	9.98	8.24
Overall CO_2 emission (10^6 ton)	27.00	22.25

In fact, larger inefficiencies are expected in mature oilfields [21]. Even considering an optimized CCGT power block in this work, previous work from Freire and Oliveira Jr [9] evidenced an average exergy efficiency gain of 9.1p.p. for a configuration similar to Case 2. However, it is noteworthy that in the referenced work the power blocks have different gas turbine models. Despite the peculiarities of the performance curves, the results obtained in this work is in line with those from the previous work and also suggest the need for an appropriate machinery selection process.

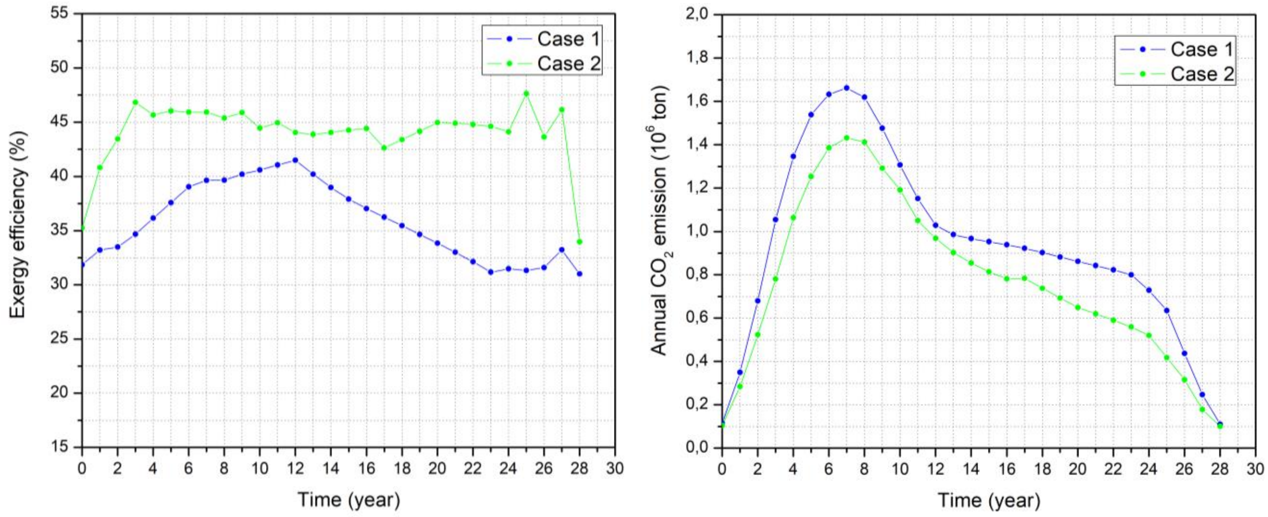

Figure 6 – Comparative exergy efficiency (left) and CO_2 emissions (right)

Despite the promising results, the commercial viability of power hubs depends on numerous factors, such as reliability not only in converting fuel energy into electricity, but also in supplying it to production platforms. Freire and Oliveira Jr [9] presented a simplified incremental financial analysis of energy hubs capable of producing part or all of the electric energy required by a set of four platforms, including a sensitivity analysis of the net present value to the taxation of CO_2 emissions. According to the authors, power hubs can be financially viable in a scenario without CO_2 taxation, although the adoption of this component radically increases the attractiveness of this solution.

5. Conclusion

Exergy efficiency and total CO_2 emission over the oilfield lifespan were used to compare the performance of utility plants in a production cluster with four platforms in the Brazilian pre-salt region. The proposed CCGT power hub increased the second-law efficiency and, thus, reduced the environmental impact of the offshore oil and natural gas production. A hybrid concept composed of a power hub equipped with optimized combined-cycle power blocks and production platforms with simple-cycle gas turbines and supplementary hot water boilers increased the lifespan average exergy efficiency by 8.2p.p. when compared to the configuration used in some commercial projects. The fuel gas consumption over the oilfield lifespan was reduced by 1.74 million ton and this reduction would avoid the emission of 4.75 million ton of carbon dioxide. This expressive environmental impact reduction is in line with operator objectives in economies with growing interest in carbon taxation.

Acknowledgments

The second author acknowledges the Brazilian National Council for Scientific and Technological Development (CNPq), grant 304935/2016-6.

Nomenclature

A boiler capacity, kW

b specific exergy, J/kg

$\dot{B}$ exergy rate, W

LHV lower heating value, MJ/kg

$\dot{m}$ mass flow rate, kg/s

NOF normalized objective function

OPEX operational expenditure, US$/MWh

P operating pressure, barg

R revenue, US$

ROCE return on capital employed, %

Abbreviations

CCGT combined-cycle gas turbine

CHP combined heat and power

FPSO Floating, production, storage and offloading

GE General Electric

HRSG heat recovery steam generator

HWB hot water boiler

MOO multi-objective optimization

SBC steam bottoming cycle

SCGT simple-cycle gas turbine

ST steam turbine

WHRU waste heat recovery unit

Greek symbols

η efficiency

Subscripts and superscripts

1,2,3 objective functions

ch chemical

el electric

ex exergy

f fuel

in inlet

kin kinetic

out outlet

ph physical

pot potential

w water

References

[1] U.S. Energy Information Administration, Offshore production nearly 30% of global crude oil output in 2015 – Available at: <https://www.eia.gov/todayinenergy/detail.php?id=28492> [accessed 27.02.2019].

[2] Anuário Estatístico Brasileiro do Petróleo, Gás Natural e Biocombustíveis: 2016. Rio de Janeiro, Brazil: National Agency of Petroleum, Natural Gas and Biofuels; 2016 Technical Report No.: ISSN 1983-5884. (in portuguese).

[3] Kloster P., Energy Optimization on Offshore Installations with Emphasis on Offshore Combined-cycle Plants. In: Proceedings of the 1999 Offshore Europe Oil and Gas Exposition and Conference; 1999 Sep 7-10; Aberdeen, Scotland. Society of Petroleum Engineers Inc.

[4] Nguyen T.-V., Tock L., Breuhaus P., Maréchal F., Elmegaard B. Oil and gas platforms with steam bottoming cycles: System integration and thermoenvironomic evaluation. Applied Energy 2014;131:222–237.

[5] Følgesvold E., Skjefstad H. S., Riboldi L., Nord L. O. Combined heat and power plant on offshore oil and gas installations. Journal of Power Technologies 2017; 97(2):117–126.

[6] Nord L. O., Martelli E., Bolland O. Weight and power optimization of steam bottoming cycle for offshore oil and gas installations. Energy 2014; 76:891-898.

[7] Riboldi L. Nord L. O. Lifetime Assessment of Combined-cycles for Cogeneration of Power and Heat in Offshore Oil and Gas Installations. Energies 2017; 10(6), 744.

[8] Vidoza J. A., Andreasen J. G., Haglind F., Reis M. M. L, Gallo W., Design and optimization of a power hub for Brazilian off-shore oil production units. Energy 2019; 176:656-666.

[9] Freire R. L. A., Oliveira Jr S., Technical and economic assessment of power hubs for offshore oil and gas application. In: Proceedings of the ECOS 2019 – The 32nd International Conference on Efficiency, Cost, Optimization, Simulation and Environmental Impact of Energy Systems; 2019 Jun 23-28; Wroclaw, Poland.

[10] Silva J. A. M, de Oliveira Jr S. Unit exergy cost and CO_2 emissions of offshore petroleum production. Energy 2018;147:757-766.

[11] Gallo W. L. R., Gallego A. G., Acevedo V. L., Dias R., Ortiz H. Y., Valente B. A., Exergy analysis of the compression systems and its prime movers for a FPSO unit. Journal of Natural Gas Science and Engineering 2017;44:287–298.

[12] http://www.wmo.int/pages/prog/wcp/wcdmp/GCDS_1.php [accessed 29.09.2019].

[13] http://www.inmet.gov.br/portal/index.php?r=clima/graficosClimaticos [accessed 29.09.2019].

[14] Thermoflow Inc. GT Pro and GT Master Version 28.2. 2019.

[15] Liu Z., Karimi I. A. Simulating combined cycle gas turbine power plants in Aspen Hysys. Energy Conversion and Management 2018; 171:1213-1225.

[16] Yang X.-S., Nature-inspired optimization algorithms. Amsterdam: Elsevier; 2014.

[17] Pintarič Z. N., Kravanja Z. Towards Outcomes-Based Education of Computer-Aided Chemical Engineering. In: Proceedings of the ESCAPE 26 – The 26th European Symposium on Computer Aided Process Engineering; 2016 Jun 12-15; Portorož, Slovenia.

[18] Mathworks, Matlab®, Version R2019a; 2019.

[19] Bosch Industriekessel GmbH. Efficient technology for major tasks. Hot water boilers. – Available at: <https://www.bosch-thermotechnology.com/> [accessed 03.01.2020].

[20] Szargut J., Morris D.R., Steward F.R., Exergy analysis of thermal, chemical and metallurgical processes. New York: Hemisphere Publ. Corp; 1988.

[21] Nguyen T.-V., Jacyno T., Breuhaus P., Voldsund M., Elmegaard B. Thermodynamic analysis of an upstream petroleum plant operated on a mature field. Energy 2014;68:454-469.